

Received August 27, 2019, accepted September 18, 2019, date of current version December 13, 2019.

Digital Object Identifier 10.1109/ACCESS.2019.2949247

Optimal Massive MIMO Detection for 5G Communication Systems via Hybrid n-Bit Heuristic Assisted-VBLAST

MUHAMMAD HAROON SIDDIQUI¹, KIRAN KHURSHID¹, IMRAN RASHID¹,
ADNAN AHMED KHAN², AND KHUBAIB AHMED³

¹Department of Electrical Engineering, National University of Sciences and Technology, Islamabad, Pakistan

²Department of Computer Software Engineering, National University of Sciences and Technology, Islamabad, Pakistan

³Department of Physics, COMSATS University, Islamabad, Pakistan

Corresponding author: Kiran Khurshid (kirankhurshid@mcs.edu.pk)

ABSTRACT Being increasingly spectral and energy efficient, massive multiple-input multiple-output (MIMO) is envisaged as a potential technology for fifth generation (5G) wireless communication networks. Radio spectrum has become a scarce resource in wireless communications and consequently imposes excessive cost on the high data rate transmission. Several linear and non linear detection techniques such as Zero-Forcing (ZF), Minimum Mean Square Error (MMSE), and Vertical Bell-Labs Layered Space Time (VBLAST) have been introduced. The purpose of such schemes is to mitigate the signal detection problems which are based on trade-offs between the bit error rate (BER) performance and computational complexities. The challenge in the design of massive-MIMO systems is developing less complex and efficient detection algorithms. The problem in building a receiver for massive-MIMO is to de-correlate the spatial signatures on the receiver antenna array. In this paper, we propose a novel algorithm viz: Hybrid n-Bit Heuristic Assisted-VBLAST (HHAV) to perform an optimum decoding. We have simulated this structure in dynamic Rayleigh fading channel. We have also evaluated the AMP algorithm with two threshold functions which include AMP with ternary distribution (AMPT) and AMP with Gaussian distribution (AMPG). Numerical results confirm that HHAV algorithm performs significantly better than the in vogue aforementioned detection systems as introduced in recent years.

INDEX TERMS Massive MIMO, VBLAST, approximate message passing, AMPT, AMPG, 5G.

I. INTRODUCTION

Nowadays in wireless communication systems, massive MIMO has become the subject of an extensive research due to its potential to support higher data rate as compared to their counterpart single-input single-output (SISO) [1]–[3]. Hence, massive-MIMO systems with tens to hundreds of antennas at the base-station (BS) have gained the attention of researchers [2], [4]–[11]. A few hurdles, however, remain to be overcome to achieve optimum advantages offered by massive MIMO systems. One of them is to model a less computational and reliable detection system without compromising performance. The motivation to consider massive MIMO systems is their potential to meet the growing demands for higher throughput as the volume, velocity, and variety of

data due to exponential augmentation in mobile users and communication networks [12]. The ever-increasing number of users in various mobile networks along with the additional enabling connectivity of the mobile services [13], [14], has necessitated the 5G technologies [15]. The aim of 5G is to provide the much-needed capacity, increased data rates, reduced latency, and improved quality of service as compared to previous technologies.

In massive-MIMO, detection is a complicated process. It requires an extensive search over the space in order to find the closest received symbols in terms of euclidean distances for an optimal solution. However, these procedures are rendered unfeasible for larger systems such as massive MIMO systems. In recent years, several architectures have been introduced for large scale systems which include Maximum Likelihood (ML) detection scheme, ZF, MMSE, and VBLAST. Efficient performance by the aforementioned

The associate editor coordinating the review of this manuscript and approving it for publication was Liang Yang.

systems, is qualified by an impossibly conducive environment and conditions. In ML detection, complexity increases with increase in number of transmit antennas. ZF is a linear detection scheme and is relatively simpler, however, it amplifies the noise due to the large gain of ZF filter especially at frequencies where the received signal is very weak. MMSE equalizer works like ZF when SNR has higher value, whereas MMSE considers noise and signal variance when the SNR has lower values to avoid noise amplification. Both ZF and MMSE (linear detectors) are quite simple to implement as compared to ML detection scheme with inferior BER performances.

Vertical-Bell Laboratories Layered Space-Time (VBLAST) scheme exhibited a spectral efficiency as high as 40 bits/s/Hz during its implementation on MIMO in real time scenario [16]. VBLAST is uncomplicated as compared to many other proposed schemes with capacity to achieve a high spectral efficiency of MIMO channels [16]. Unlike BLAST decoder where symbols are decoded in their natural order, VBLAST employs ordered successive interference cancellation (OSIC) [17]. In OSIC the symbols are arranged with respect to the SNR. Symbols with highest SNR are at the top with decreasing SNR towards the bottom. Overall the performance of VBLAST decoder is better than the ZF decoder with high computational complexity.

To meet the requirements of transferring enormous size of data to ever-increasing users instantaneously, a number of schemes have been introduced to mitigate the problems and enhance the efficiency of existing solutions. Using precoding of the transmitted symbols based upon the knowledge of channel state information (CSI), may improve time-efficiency and reliability. However, performance of precoding using plain channel inversion becomes ineffective and inefficient at all the signal-to-noise (SNRs). A precoding scheme known as vector perturbation (VP) focusing on enhancement of throughput, has been introduced in [18], [19]. The aforementioned scheme was based on Tomlinson-Harashima using modulo-lattice operations, which perturb the transmitted symbols. This scheme is efficient in achieving near-sum-capacity without using dirty paper techniques [18], [19]. The optimal solution of VP can be achieved after catering to the closest vector problem (CVP) in a lattice, which has been proved NP-complete in [20]. Since the nature of NP-complete problem is such that sphere decoding [21] is required to be used which exponentially increases the computational complexity hence, further multiplying the dimension of the problem.

Many low complexity algorithms have been introduced in literature [22]–[25]. A low-complexity iterative, approximate message passing (AMP) algorithm was proposed in [26], [27]. The performance of AMP algorithm is justified in [28], [29]. While using AMP algorithm, it is assumed that the data symbols are taken from finite discrete constellation which makes the problem complex in using the said algorithm. For instance, if the size of the constellation grows, subsequently channel matrix will become extremely

large [30]. In [31], it is shown that the calculation of the posterior mean function (known as threshold function [28]) of AMP algorithm for small values of noise variance will become numerically unstable. In [32], two threshold functions have been designed to mitigate or overcome the computational complexities of AMP algorithm. The AMP algorithm with threshold function using ternary distribution is known as AMPT whereas, the one with threshold function using Gaussian distribution is known as AMPG [32]. We have thoroughly examined the AMP algorithm and evaluated the performances of both versions with different threshold.

In this paper, we present a novel detection algorithm for massive-MIMO decoder based on heuristic search for solving the MIMO detection problem. This scheme combines the algorithm, inspired by variable depth search (VDS) [33], with the conventional VBLAST decoder. VDS is the generalized case of the local search method. The purpose is to search the current solution vis-à-vis a more efficient solution. The process is iterative in nature and the quest for local optima continues until no better solution exists. The concept of VDS was first applied by Lin and Kernighan to the traveling salesman problem (TSP) and graph partitioning problem (GPP) [34]. To the best of the authors knowledge, such investigation is unprecedented in the literature. Moreover, we prove numerically that our scheme is optimal for high SNR in terms of BER performance.

The rest of the paper is structured as follows: In Section-II, system model is presented and the performances of the existing robust detection algorithm for massive MIMO decoder is analyzed. Proposed HHAV detection algorithm is also presented in detail. Section-III presents the simulation results and compares the BER performances of the existing detection algorithm with proposed scheme. Section-IV presents future directions. In Section-V conclusions are presented.

Notations: In this paper we use upper-case and lower-case boldface letters to refer matrices and vectors respectively; $(\cdot)^H$, $(\cdot)^T$, $(\cdot)^{-1}$ and $|\cdot|$ denote conjugate transpose, transpose, inverse matrices and absolute value respectively. Real and imaginary parts are denoted by $\Re(\cdot)$ and $\Im(\cdot)$ respectively. A matrix in which each element is independent and identically distributed sampled from normal distribution is referred to as i.i.d. Gaussian matrix. Complex conjugate operation is denoted as $*$. F_a and F_c represents the mean estimation function and variance estimated function respectively. ζ and ξ are referred as threshold functions. L_i^{m+1} stands for i th element of a vector at $m^{th}+1$ iteration. $d_\psi(\cdot)$, and Ψ represent the damping function and damping factor respectively.

II. PRELIMINARIES AND SYSTEM MODEL

Consider an uplink massive MIMO system with N users terminals (UT), where each UT is equipped with single transmitting antenna, communicating with a BS, equipped with a large number of receive antennas as shown in Fig.1. Let M denote the number of BS antennas where M is in the range of tens to hundreds. Each UT encodes information bits

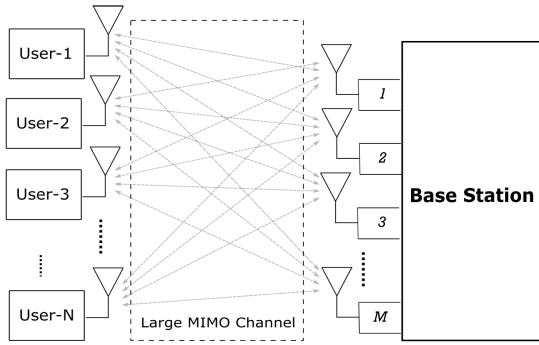


FIGURE 1. An elucidation of massive MIMO system where N indicates transmitting users and M shows the receiving antennas at the base station.

and N information bits are mapped onto the QPSK constellation diagram. After having been mapped on the constellation diagram these modulated symbols are transmitted over the massive MIMO channel, and received by the M antennas at BS. The matrices at UT ($N \times 1$ complex vector) and at BS ($M \times 1$ complex vector) are defined as x and y respectively. x is a $N \times 1$ transmit complex vector $x = [x_1, x_2, x_3, \dots, x_N]^T \in \mathcal{Q}^N$, where \mathcal{Q} stands for complex constellation. If Q represents the modulation order then $|\mathcal{Q}| = 2^Q$. Hence, $M * Q$ binary values, where $x_{i,b} \in \{1, 0\}$, $i = 1, 2, 3, \dots, M$, $b = 1, 2, 3, \dots, Q$, corresponding to the b th bit of the symbol of x_i , are associated with each transmit vector x . y is a received complex vector $y = [y_1, y_2, y_3, \dots, y_M]^T$. Assume $H_c^{(t)} \in \mathbb{C}^{(N \times M)}$ denotes the channel gain matrix in the t th channel use and h_{ij}^c denotes the complex channel gain from the j th user to the i th antenna of BS. The h_{ij}^c (channel gains) are supposed to be independent Gaussian with zero mean and variance σ_j^2 , where $\sum_j \sigma_j^2 = k$. Each σ_j^2 models the instability caused by the path loss in the received power from j th user where as in case of perfect power control the corresponding $\sigma_j^2 = 1$. Let the modulated symbol vector transmitted in the j th channel use, be denoted by $x_c^{(t)}$, where the j th element of $x_c^{(t)}$ denotes the modulation symbol transmitted by the j th user. We assume perfect synchronization, and the received vector at the BS in the t th channel use, $y_c^{(t)}$, is given by:

$$y_c^{(t)} = H_c^{(t)} x_c^{(t)} + w_c^{(t)} \tag{1}$$

where $w_c^{(t)}$ is the noise vector with the entries modeled as i.i.d. $\mathcal{CN}(0, \sigma^2)$. For convenience, the channel use index can be dropped, hence, (1) can be written as:

$$y = Hx + w \tag{2}$$

where $y \triangleq \begin{bmatrix} \Re(y_c) \\ \Im(y_c) \end{bmatrix}$, $H \triangleq \begin{bmatrix} \Re(H_c) & -\Im(H_c) \\ \Im(H_c) & \Re(H_c) \end{bmatrix}$, $x \triangleq \begin{bmatrix} \Re(x_c) \\ \Im(x_c) \end{bmatrix}$,

$w \triangleq \begin{bmatrix} \Re(w_c) \\ \Im(w_c) \end{bmatrix}$, the BS receives y and executes detection and decoding processes.

A. CHANNEL MODELING (RAYLEIGH CHANNEL MODEL)

Assume two independent random variables $\mathfrak{X} \sim \mathcal{N}(m_1, \sigma^2)$ and $\mathfrak{Y} \sim \mathcal{N}(m_1, \sigma^2)$. Assume \mathfrak{Z} denotes a complex Gaussian variable where, $\mathfrak{Z} = \mathfrak{X} + j\mathfrak{Y}$. Hence, the magnitude and phase of the random variable can be expressed a:

$$\mathfrak{R} = \sqrt{\mathfrak{X}^2 + \mathfrak{Y}^2}, \theta = \tan^{-1}\left(\frac{\mathfrak{X}}{\mathfrak{Y}}\right) \tag{3}$$

The polar elucidation of (3) is given by:

$$\mathfrak{X} = \mathfrak{R} \cos \theta, \mathfrak{Y} = \mathfrak{R} \sin \theta \tag{4}$$

Jacobian method will be used to transform an area which is given by:

$$dx dy = \ddot{r} d\ddot{r} d\vartheta \Leftrightarrow \left| \mathbb{J} \left(\begin{matrix} \ddot{r}, \vartheta \\ x, y \end{matrix} \right) \right| = \frac{1}{\ddot{r}} \tag{5}$$

Joint distribution of \mathfrak{R} and ϑ can be expressed by using Jacobian method which gives:

$$\begin{aligned} \mathfrak{F}_{\mathfrak{R}, \Psi}(\ddot{r}, \vartheta) &= \frac{\ddot{r}}{2\pi\sigma^2} \exp\left(-\frac{\ddot{r}^2 + s^2}{2\sigma^2}\right) \\ &\times \exp\left(-\ddot{r} \frac{m_1 \cos\vartheta + m_2 \sin\vartheta}{2\sigma^2}\right) \ddot{u}(\ddot{r}), \quad \vartheta \in (-\pi, \pi) \end{aligned} \tag{6}$$

$\mathcal{B}_0(x)$ is the modified zeroth order Bessel function which can be defined as:

$$\mathcal{B}_0(x) = \frac{1}{2\pi} \int_0^{2\pi} e^{-x \cos\vartheta} d\vartheta \tag{7}$$

s is referred as the non-centrality parameter of faded envelope and is given by:

$$s = \sqrt{m_1^2 + m_2^2} \tag{8}$$

The power in the faded envelope produced by the means of X and Y is known as Rice factor \mathcal{R} and is defined as:

$$\mathcal{R} = \frac{m_1^2 + m_2^2}{2\sigma^2} = \frac{s^2}{2\sigma^2} \tag{9}$$

By integrating (9) over $\vartheta \in (-\pi, \pi)$ from $\mathfrak{F}_{\mathfrak{R}, \Psi}(\ddot{r}, \vartheta)$, marginal distribution is obtained over the envelope:

$$\mathfrak{F}_{\mathfrak{R}}(\ddot{r}) = \frac{\ddot{r}}{\sigma^2} \exp\left(-\frac{\ddot{r}^2 + s^2}{2\sigma^2}\right) \mathcal{B}_0\left(\frac{\ddot{r}s}{\sigma^2}\right) \ddot{u}(\ddot{r}) \tag{10}$$

For the phase, marginal distribution depends on ϑ , hence it can be found by integrating only \mathfrak{R} out of joint distribution which is given by:

$$\begin{aligned} \mathfrak{F}_{\Psi}(\vartheta) &= \frac{1}{2\pi} \exp\left(-\frac{s^2}{2\sigma^2}\right) \frac{\mathcal{M}}{2\pi\sigma^2} \exp\left(-\frac{\mathcal{M}^2 + s^2}{2\sigma^2}\right) \\ &\times \mathcal{G}\left(-\frac{\mathcal{M}}{\sigma}\right), \quad \theta \in (-\pi, \pi) \end{aligned} \tag{11}$$

where \mathcal{M} is defined as:

$$\begin{aligned} \mathcal{M} &= m_1 \cos \vartheta + m_2 \sin \vartheta \\ &= \sqrt{m_1^2 + m_2^2} \cos[\vartheta + \cos^{-1}(\frac{m_1}{m_2})], \end{aligned} \quad (12)$$

and $\mathcal{G}(x)$ is defined as:

$$\mathcal{G}(x) = \frac{1}{\sqrt{2\pi}} \int_x^\infty \exp(-\frac{y^2}{2}) dy \quad (13)$$

where $\mathcal{G}(x)$ expresses the normalized Gaussian tail probability function.

When

$$\mathcal{R} = \frac{m_1^2 + m_2^2}{2\sigma^2} = \frac{s^2}{2\sigma^2} = 0 \quad (14)$$

then the marginal for the phase is:

$$\mathfrak{F}_\Psi(\vartheta) = \begin{cases} \frac{1}{2\pi} & \vartheta \in (-\pi, \pi) \\ 0 & \text{otherwise} \end{cases} \quad (15)$$

The phase of \mathfrak{Z} is uniformly distributed, whereas PDF of Rayleigh distribution is given by

$$\mathfrak{F}_{\mathfrak{R}}(\ddot{r}) = \begin{cases} \frac{\ddot{r}}{\sigma^2} \exp(-\frac{\ddot{r}^2}{2\sigma^2}) & 0 \leq \ddot{r} \leq \infty \\ 0 & \ddot{r} < 0 \end{cases} \quad (16)$$

B. MULTIUSER ENCODING AT TRANSMITTER SIDE

Each user $n = 1, 2, 3, \dots, N$, follows the information bit sequences b_k using QPSK modulation. Symbols are encoded before transmission. The encoded symbol is referred to as $x(n, i, t)$, where $i = 1, 2, \dots, k$ represents number of each symbol and t shows particular time slot [35]. As an example we have shown the transmission sequences of two users with one antenna each in table1. The signal transmitted by the first user at first time slot is represented by $x_{1,1,1}$ and during second time slot it is represented by $x_{1,2,2}^*$. Similarly, $x_{2,1,1}$ and $x_{2,2,2}^*$ are the signals transmitted by the second user during first and second time slot respectively.

TABLE 1. Structure of transmission order for two users with one transmit antenna each.

USER-1 (Time Slot)	ANTENNA-1
t_1	$x_{1,1,1}$
t_2	$x_{1,2,2}^*$
USER-2 (Time Slot)	ANTENNA-2
t_1	$x_{2,1,1}$
t_2	$x_{2,2,2}^*$

C. MULTIPLE ACCESS CHANNEL DECODING

Symbols received from the users (in this section we will show the working for two users only) at t_1 where t_1 denotes first time slot, is given by:

$$\mathcal{R}^{t_1} = H^{t_1} \mathfrak{X}^{t_1} + \mathcal{W}^{t_1} \quad (17)$$

where, $\mathcal{R}^{t_1} = \begin{bmatrix} r_1^1 \\ r_1^1 \\ \vdots \\ r_{K_R}^1 \end{bmatrix}$ is received vector at t_1 with elements r_l^t for $t = 1$ and $l = 1, 2, 3, \dots, K_R$,

$$H^{t_1} = \begin{bmatrix} h_{111} & h_{211} & \dots & h_{N11} \\ h_{121} & h_{221} & \dots & h_{N21} \\ \vdots & \vdots & \ddots & \vdots \\ h_{1K_R1} & h_{2K_R1} & \dots & h_{NK_R1} \end{bmatrix}$$

is the realization of the channel matrix at first time slot. Consider each user with \mathfrak{J} numbers of antennas then realization of the channel matrix will be H^{t_1} , as shown at the bottom of this page, is the transmitted vector with the elements $x(N, i)$

$$H^{t_1} = \begin{bmatrix} h_{1111} & \dots & h_{111\mathfrak{J}} & h_{211} & \dots & h_{211\mathfrak{J}} & \dots & h_{N11} & \dots & h_{N1\mathfrak{J}} \\ h_{1211} & \dots & h_{121\mathfrak{J}} & h_{221} & \dots & h_{221\mathfrak{J}} & \dots & h_{N21} & \dots & h_{N2\mathfrak{J}} \\ \vdots & \ddots & \vdots & \vdots & \ddots & \vdots & \ddots & \vdots & \ddots & \vdots \\ h_{1K_R11} & \dots & h_{1K_R1\mathfrak{J}} & h_{2K_R1} & \dots & h_{2K_R1\mathfrak{J}} & \dots & h_{NK_R1} & \dots & h_{NK_R1\mathfrak{J}} \end{bmatrix}$$

$$\mathfrak{X} = \begin{bmatrix} x_{1,1} \\ x_{1,2} \\ x_{2,1} \\ x_{2,2} \\ \vdots \\ x_{N-1,1} \\ x_{N,2} \end{bmatrix}$$

which is the signal $x(n, i, t)$ for i th signal of the n th user, and

$$\mathcal{W}^{t1} = \begin{bmatrix} w_1^1 \\ w_1^1 \\ \vdots \\ w_{K_R}^1 \end{bmatrix} \text{ is a noise vector at } t1.$$

Similarly, signal received at $t2$ is given by:

$$\mathcal{R}^{t2} = H^{t2}\mathbb{X}^{t2} + \mathcal{W}^{t2} \tag{18}$$

where, $\mathcal{R}^{t2} = \begin{bmatrix} r_1^{2*} \\ r_1^{2*} \\ \vdots \\ r_{K_R}^{2*} \end{bmatrix}$ is the received signal during the second

time slot with elements r_l^t for $t = 2$ and $l = 1, 2, 3, \dots, K_R$,

$$H^{t2} = \begin{bmatrix} h_{112}^* & h_{212}^* & \dots & h_{K12}^* \\ h_{112}^* & h_{222}^* & \dots & h_{K22}^* \\ \vdots & \vdots & \ddots & w_{K3} \\ h_{1K_R2}^* & h_{2K_R2}^* & \dots & h_{N_{K_R2}}^* \end{bmatrix}$$

is the realization of the channel matrix at second time slot and

$$\mathcal{W}^{t2} = \begin{bmatrix} w_1^{2*} \\ w_1^{2*} \\ \vdots \\ w_{K_R}^{2*} \end{bmatrix} \text{ is a noise vector at } t2. \text{ The expression of}$$

composite received signal \mathcal{R}_k of both (two) time slots is given by:

$$\mathcal{R}_k = H_k\mathbb{X}_k + \mathcal{W}_k \tag{19}$$

where, $\mathcal{R}_k = \begin{bmatrix} \mathcal{R}^{t1} \\ \mathcal{R}^{t2} \end{bmatrix}$, $H_k = \begin{bmatrix} H^{t1} \\ H^{t2} \end{bmatrix}$, and $\mathcal{W}_k = \begin{bmatrix} \mathcal{W}^{t1} \\ \mathcal{W}^{t2} \end{bmatrix}$ The estimation of transmitted signal $\hat{\mathcal{R}}_k$ is:

$$\begin{aligned} \hat{\mathcal{R}}_k &= H^{\mathbb{H}}\mathcal{R}_k \\ &= H^{\mathbb{H}}H_k\mathbb{X}_k + H^{\mathbb{H}}\mathcal{W}_k \\ &= H^{\mathbb{H}}H_k\mathbb{X}_k + H^{\mathbb{H}} + \hat{\mathcal{W}}_k \end{aligned} \tag{20}$$

D. THE AMP ALGORITHM

The optimal detector in massive MIMO systems is rendered extremely complex due to the challenging detection of an individual signal from the composite received signal with a large system limit. The approximate message passing (AMP) algorithm has become an attractive area for research especially in massive MIMO systems due to its inherent reduced complexity. To counter the problem of complexity with a large system limit, AMP algorithm has been used by researchers for detection in massive MIMO systems. The AMP algorithm is used efficiently for reconstruction of original signal in compress sensing [36]. AMP algorithm is less complex and its implementation is realizable, however,

the convergence of the algorithm is not guaranteed especially in case of finite size system. Nonetheless, to facilitate the convergence of the algorithm many mechanisms including damping [37] and estimation function to fixed point format [38], have been proposed. We also simulated the AMP algorithm, as summarized in Algorithm 1, where, \hat{x}_i^{m+1} stands for i th element of an estimated vector at the m th iteration and v_i^{m+1} represents i th element of a vector at the m th + 1 iteration, to compare the result with our proposed algorithm in terms of BER (for detailed derivation of the algorithm we refer to [39]). It is noteworthy that desired results from AMP algorithm can only be obtained if it is implemented with certain threshold functions [23] carefully designed as per the specification of coefficient vector x .

Algorithm 1 The AMP Algorithm

- 1 Initialization:
 - 2 Set $\hat{x}^0 = 0, \sum^0 = \sigma_x^2, v^0 = 1$
 - 3 **for** $m = 1, 2, \dots$, **do**
 - 4 $V_j^{m+1} = \sum_i |H_{j,i}|^2 v_i^m$
 - 5 $V = \sigma_n^2 + V - j^m$
 - 6 $D = y_j - w_j^m$
 - 7 $w_j^{m+1} = \sum_{i=1}^M H_{j,i} \hat{x}_i^m - \frac{D}{V} \sum_i |H_{j,i}|^2 v_i^m$
 - 8 $D'_{new} = y_j - w_j^m$
 - 9 $V'_{new} = \sigma_n^2 + V_j^{m+1}$
 - 10 $D'_{new} = d_{\Psi}(D, D'_{new}, \Psi)$
 - 11 $V'_{new} = d_{\Psi}(V, V'_{new}, \Psi)$
 - 12 $\sum_i^{m+1} = [\sum_j \frac{|H_{j,i}|^2}{V_{new}^{m+1}}]^{-1}$
 - 13 $L_i^{m+1} = \hat{x}_i^m + \frac{\sum_j H_{j,i} \frac{D'_{new}^{m+1}}{V_{new}^{m+1}}}{\sum_j \frac{|H_{j,i}|^2}{V_{new}^{m+1}}}$
 - 14 $\hat{x}_i^{m+1} = F_a(R_i^{m+1}, \sum_i^{m+1})$
 - 15 $v_i^{m+1} = F_c(R_i^{m+1}, \sum_i^{m+1})$
 - 16 **end for**
-

1) AMPT

In AMP algorithm [23] ZF/SIC is used for initial guess of maximal error distance which is practically very close to small scale sphere decoding and certain probabilities also exist in which large dimensions contain slight error distance. Ternary distribution is used [32] for such scenarios. Empirical study has also proved that maximum portion of errors can be removed by using ternary distribution $\{-1, 0, 1\}$ for $PX(x_q)$. The expressions of its threshold functions have already been proved in [31], however, for $Y = X + W$ where $X \sim PX(x) = (1 - \epsilon)\delta(x) + \epsilon/2\delta(x - 1) + \epsilon/2\delta(x + 1)$, $W \sim N(0, s)$,

the final expressions are as follow:

$$\zeta_{\epsilon}(r, s) \triangleq \mathbb{E}(X|Y = r) = \frac{\sinh(r/s)}{(1 - \epsilon)/\epsilon e^{1/(2s)} + \cosh(r/s)} \quad (21)$$

$$\xi_{\epsilon}(r, s) \triangleq \mathbb{V}(X|Y = s) = \frac{(1 - \epsilon)/\epsilon e^{1/(2s)} + \cosh(r/s) + 1}{((1 - \epsilon)/\epsilon e^{1/(2s)} + \cosh(r/s))^2} \quad (22)$$

The computational complexity is lower since these threshold functions are in closed forms. We also simulate AMPT algorithm using (21) and (22) to evaluate the performance.

2) AMPG

For instance [32] shows that maximum error distance $\max_i |\hat{x}_i - x_i^{CVP}|$, where \hat{x} is sub-optimal candidate and $x^{CVP} = \arg \min \|y - Hx\|^2$, will increase with the growing system dimensions, hence it admits a discrete Gaussian distribution. The AMP algorithm [32] is referred to as AMPG which uses linear estimation based on continuous Gaussian distribution. Let $Y = r$ from model $Y = X + W$ where $X \sim PX(x) = \varrho\sigma_g(x)$, $W \sim N(0, s)$. The threshold functions have been proved in details in [32] whereas, the final expressions are as follow:

$$\zeta_{\epsilon}(r, s) = \frac{1}{S_k} \sum_{l=-k}^k l e^{-\frac{l^2}{2\sigma_g^2} - \frac{(1-r)^2}{2s}} \quad (23)$$

$$\xi_{\epsilon}(r, s) = \frac{1}{S_k} \sum_{l=-k}^k (l - \zeta_g(r, s))^2 e^{-\frac{l^2}{2\sigma_g^2} - \frac{(1-r)^2}{2s}} \quad (24)$$

We simulate and evaluate the result of AMPG algorithm using (23) and (24) for threshold functions in section III.

E. THE VBLAST DETECTOR

The strategy of “divide-and-conquer” is adopted instead of decoding all the symbols concurrently to lessen the computational complexity at receiver end. In this approach, the strongest symbol is decoded first and its effect is cancelled from all received symbols. Furthermore, the next strongest symbol is detected in the same manner and its effect from all received symbols is eliminated. This algorithm continues till the time the last received symbol is detected and its effect is eliminated. VBLAST algorithm [40] works efficiently in massive MIMO where $M > N$. The three steps of algorithm include ordering, interference cancellation, and Interference nulling. The OSIC algorithm is summarized in Algorithm 2.

The pseudo inverse of H is represented as H^+ . $(U_i)_j$ is the j^{th} row of U_i . $(H)_{k_i}$ is the k_i^{th} column of H . $(H)_{\hat{k}_i}^+$ is referred as the ZF resultant matrix by zero forcing, whereas $Q_z(\cdot)$ represents a slicer. This algorithm first carries out the ordering of the received symbols in terms of SNR from strongest to the weakest. Subsequently, it statistically determines the first symbol after the process of nulling. Finally, before the computation of new inverse channel matrix, the effect of the strongest detected symbol is eliminated by canceling out the coefficient of H . This process is recursive and continues to decode the received symbols. The aforementioned VBLAST

Algorithm 2 Ordered Successive Interference Cancellation

```

1 initialization  $i = 1, U_1 = H^+$ ,
                 $k_i = \arg \min_j \|(U_i)_j\|^2$ 
for iteration 1 do
2    $y_{k_i} = (U_i)_{k_i} y_i$ 
3    $\hat{x}_{k_i} = (Q)_z(y_{k_i})$ 
4    $y_{i+1} = y_i - \hat{x}_{k_i}(H)_i$ 
5    $U_{i+} = (H)_{\hat{k}_i}^+$ 
6
                 $k_{i+1} = \arg \min_{(j) \notin \{k_1, k_2, \dots, k_i\}} \|(U_{i+1})_j\|^2$ 
7    $i \leftarrow i + 1$ 
8 end for

```

algorithm adopts ZF approach. The minimum noise variance $\|(H^+)_j\|^2 N_0$ is employed for ordering of the symbols.

F. HYBRID N-BIT HEURISTIC ASSISTED-VBLAST DETECTION ALGORITHM (HHAV)

Heuristics are based on approximate schemes to find best possible outcome which may or may not be optimally corresponding to the complex combinatorial optimization challenge in polynomial-time. The heuristic methods have two major classifications such as construction method and local search method. The former generates results without any initial guess or solution. It is an iterative process which adds random solution components to the preliminary empty solution until the process is completed. On the contrary, local search schemes commence with certain initial findings. It is also an iterative process which keeps on improving the current outcome by searching within a pre-designated neighbourhood. A neighborhood structure is used to specify the outcomes neighbourhood. It is believed, however, that better solution exists as compared to the previously estimated result. HHAV algorithm is observed to be efficient in searching a better solution. HHAV algorithm search for the best possible solution by adding a small offset value to the magnitude of the received estimated symbol from VBLAST algorithm on the complex plane. The system structure of proposed scheme is shown in Fig.2. Firstly, the offset value is added to the magnitude of the received estimated complex symbol. The same offset value is added to the real part thereafter and finally to the imaginary part of the received estimated complex symbol. Hence, three more symbols on the complex plane are computed by using aforementioned method. The primary aim is to seek the number of sufficient $(n - bit)$ (four neighbours are generated in this proposed scheme) neighbourhood while maintaining the reasonable complexity and computation time. Functions (31)-(34) are used to find out the minimum Euclidean distances. First \hat{S}_R is computed

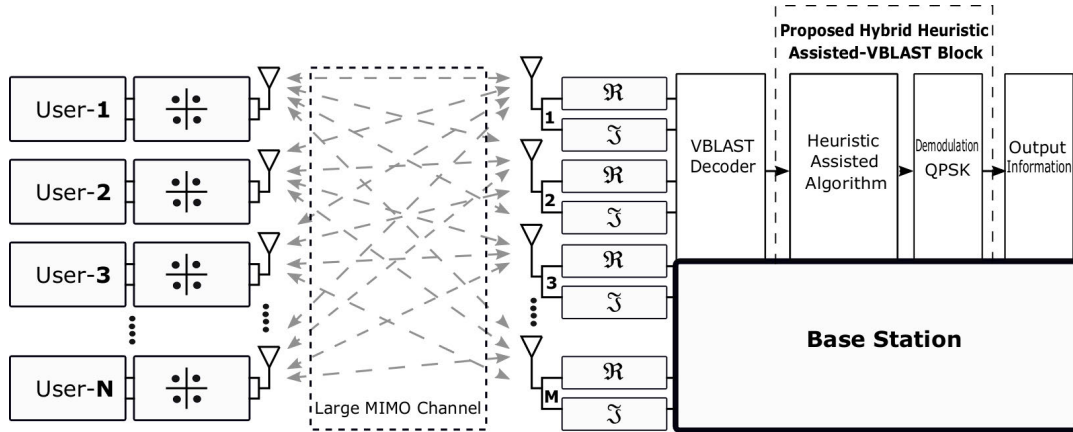


FIGURE 2. System structure of the proposed scheme.

Algorithm 3 Proposed Hybrid n-Bit Heuristic Assisted VBLAST

Data: $\{y_1, y_2, \dots, y_k\}, \{H_1, H_2, \dots, H_k\}, \{x_1, x_2, \dots, x_k\}, N_{itr}, N_t$

Result: $\{\hat{x}_1, \hat{x}_2, \dots, \hat{x}_k\}$

1 **initialization** $\hat{x} = X_i$ where $i = 1, 2, 3, \dots, k$; *ith* residual $a_i = y_i \setminus H_i x_i \forall i$;

2 **for iteration 1 : N_{itr} do**

3 $y_{k_i} = (U_i)_{k_i} y_i$

4 $\hat{S}_{R_{k_i}} = (Q)_z(y_{k_i})$

5 $y_{i+1} = y_i - \hat{x}_{k_i}(H)_i$

6 $U_{i+} = (H)_{k_i}^+$

7

$$k_{i+1} = \underset{(j) \notin \{k_1, k_2, \dots, k_i\}}{\text{arg min}} \|(U_{i+1})_j\|^2$$

8 **for $j = 1 : N_t$ do**

9 $\hat{S}_{R1j} = \sqrt{(\ln |\hat{S}_R|)^2 + (\theta)^2} + \psi$

10 $\hat{S}_{R2j} = |\Re(\hat{S}_R)| + \psi$

11 $\hat{S}_{R3j} = |\Im(\hat{S}_R)| + \psi$

12 **end for**

13 **for $i = 1 : 3$ do**

14 **for $a = 1 : \hat{S}_{Rij} + 1$ do**

15 | Euclidean distance = $E(a) = \|y - H \hat{S}_{Rij}\|^2$

16 **end for**

17 $\hat{x}_1 = \min E(a)$

18 **end for**

19 $i \leftarrow i + 1$

20 **end for**

Let's suppose \hat{S}_R is the estimated complex received symbol through VBLAST algorithm and is defined by:

$$\hat{S}_R = |\hat{S}_R| e^{i\theta} \tag{25}$$

Taking the natural log of (25) gives:

$$\ln \hat{S}_R = \ln |\hat{S}_R| + i\theta \tag{26}$$

where $\ln |\hat{S}_R|$ is the real part and $i\theta$ is an imaginary part. The magnitude is given by:

$$\sqrt{(\ln |\hat{S}_R|)^2 + (\theta)^2} \tag{27}$$

Let's suppose $\hat{S}_{R1}, \hat{S}_{R2}, \hat{S}_{R3}$ are three estimated symbols received after adding small offset value ψ and are defined as under:

$$\hat{S}_{R1} = \sqrt{(\ln |\hat{S}_R|)^2 + (\theta)^2} + \psi \tag{28}$$

$$\hat{S}_{R2} = |\Re(\hat{S}_R)| + \psi \tag{29}$$

$$\hat{S}_{R3} = |\Im(\hat{S}_R)| + \psi \tag{30}$$

$\hat{S}_R, \hat{S}_{R1}, \hat{S}_{R2},$ and \hat{S}_{R3} are four estimated points or symbols on complex plane. The original points on the constellation are known, hence the smallest euclidean distance of the estimated points from the original points on the constellation will give the best solution for the desired symbol. Let $\mathcal{S}_{O_{\Re, \Im}}$ is the original point on the constellation. The euclidean distances $\bar{\partial}_{dist(\cdot)}$ of the estimated points from the original point $\mathcal{S}_{O_{\Re, \Im}} = |\mathcal{S}_{O_{\Re, \Im}}| e^{i\theta}$ can be given by:

$$\bar{\partial}_{dist1} = \|\hat{S}_R - \mathcal{S}_{O_{\Re, \Im}}\|^2 \tag{31}$$

$$\bar{\partial}_{dist2} = \|\hat{S}_{R1} - \mathcal{O}_{\Re, \Im}\|^2 \tag{32}$$

$$\bar{\partial}_{dist3} = \|\hat{S}_{R2} - \mathcal{O}_{\Re, \Im}\|^2 \tag{33}$$

$$\bar{\partial}_{dist4} = \|\hat{S}_{R3} - \mathcal{O}_{\Re, \Im}\|^2 \tag{34}$$

Finally our desired received symbol $\hat{\mathcal{R}}$ will be :

$$\hat{\mathcal{R}} = \min(\bar{\partial}_{dist1}, \bar{\partial}_{dist2}, \bar{\partial}_{dist3}, \bar{\partial}_{dist4}) \tag{35}$$

Fig.3 shows the flowchart of the proposed HHAV detection algorithm.

and then a *ML* search around the neighbourhood of \hat{S}_R is performed. The resultant values (after adding offset) are converted into bits to find the neighbours of the received symbol. A neighbour list is maintained by each of the N_t symbols to search simultaneously over a specific constellation.

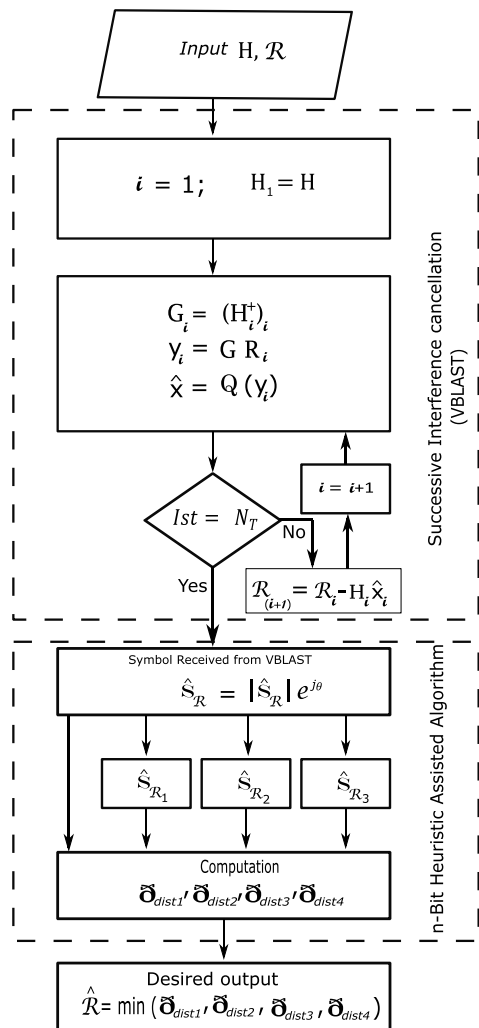


FIGURE 3. Flowchart of the proposed HHAV detection algorithm.

G. COMPLEXITY OF HHAV

The complexity of an algorithm is evaluated by considering the number of floating-point operations (flops). The complexity of an AMP algorithm is $O(mnT)$ flops whereas the complexity of ZF/SIC is $O(mn^2)$ flops [32]. HHAV is a heterogeneous algorithm, hence its complexity is considered in conjunction with VBLAST (ZF/SIC) algorithm. The big- O notation excludes the coefficients and lower order terms. HHAV algorithm searches the best solution within specific reduced constellation, hence its computational complexity will remain $O(mn^2)$.

III. SIMULATIONS

We consider an uplink massive MIMO system with $N = 16, 32, 64$ independent users equipped with single antenna, whereas the receiver is equipped with $M = 32, 64, 128$ receiving antennas. The modulation scheme considered for our simulations is QPSK. We generate a random channel matrix H and random transmit vector x . The channel model is assumed to be Rayleigh fading, whereas the symbols in

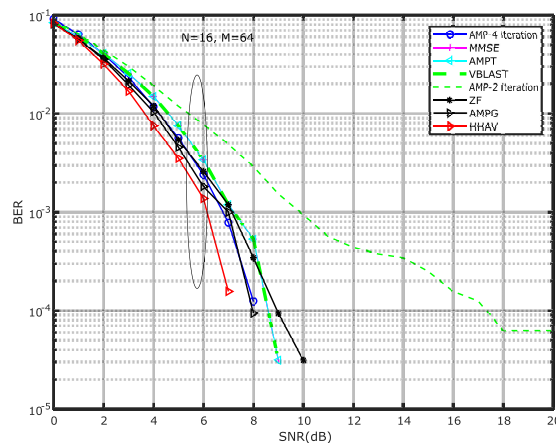


FIGURE 4. An illustration of BER performance of decoding algorithms in a 16 x 64 Massive MIMO system with QPSK modulation scheme.

random vector are uncorrelated. The energy per bit to noise power spectral density ratio is defined as:

$$\frac{E_b}{N_0} = \frac{E_s}{N_0} + 10 \log_{10} \frac{M}{RNQ}, \tag{36}$$

where, $\frac{E_s}{N_0}$ is the average energy per transmitted symbol.

In this section the BER performance of the proposed hybrid decoding scheme is compared and analyzed with other existing schemes through Monte Carlo simulations. The performances of the conventional linear and nonlinear decoders such as ZF, MMSE and VBLAST are examined. The impacts of AMP algorithm vis-à-vis threshold functions AMPG and AMPT [23], [32] are also studied.

First, Fig. 4 illustrates the SNR(dB) versus BER performances of various algorithms using the antenna configuration $N \times M = 16 \times 64$ with modulation QPSK. As shown in Fig. 4, HHAV performs better than other algorithms and this performance become more palpable with increase in SNR(dB). Performances of AMP(G) and AMP (AMP-4 iteration) are equal. Likewise, the BER values of AMP(T) and VBLAST also remains comparable.

Fig. 5 presents the comparison of SNR(dB) versus BER performances of existing algorithms using antenna configuration 32×64 with QPSK modulation scheme. HHAV outperforms the other algorithms with considerable margin. It is also evident from the results that BER improvement, as offered by the proposed algorithm, gets more pronounced as the system configuration grows. In this scenario, AMP (AMP-4 iteration), AMP(T), and VBLAST exhibit identical results, whereas, BER value of AMP(G) becomes constant when it reaches closer to 10^{-4} value.

To investigate the robustness of the proposed hybrid scheme we considered a high-dimensional MIMO system with $N = 32$ users and $M = 128$ antennas at the receiver. In Fig. 6, our results show that in 32×128 configuration, our proposed scheme performs better than the rest of the algorithms in terms of SNR(dB) versus BER. Performance of AMP(T) is better than AMP (AMP-4 iteration) and AMP(T),

TABLE 2. Comparison of BER performances of different schemes in terms of number of users and number of receiving antennas.

Modulation QPSK	HHAV		AMP (4-iteration)		AMP(G)		AMP(T)		VBLAST	
	BER	SNR	BER	SNR	BER	SNR	BER	SNR	BER	SNR
$N = 16, M = 64$	10^{-1}	0dB	10^{-1}	0dB	10^{-1}	0dB	10^{-1}	0dB	10^{-1}	0dB
$N = 16, M = 64$	10^{-2}	3dB	10^{-2}	3.7dB	10^{-2}	3.6dB	10^{-2}	4dB	10^{-2}	4dB
$N = 16, M = 64$	10^{-3}	6dB	10^{-3}	6.5dB	10^{-3}	6.6dB	10^{-3}	7.3dB	10^{-3}	7.5dB
$N = 16, M = 64$	10^{-4}	7.1dB	10^{-4}	8.1dB	10^{-4}	8dB	10^{-4}	9.2dB	10^{-4}	9.4dB
$N = 32, M = 64$	10^{-1}	6.5dB	10^{-1}	7.5dB	10^{-1}	6.5dB	10^{-1}	6.5dB	10^{-1}	6.4dB
$N = 32, M = 64$	10^{-2}	11dB	10^{-2}	12dB	10^{-2}	11.8dB	10^{-2}	11.8dB	10^{-2}	11.7dB
$N = 32, M = 64$	10^{-3}	12.5dB	10^{-3}	14.1dB	10^{-3}	14.8dB	10^{-3}	14.3dB	10^{-3}	14.2dB
$N = 32, M = 64$	10^{-4}	13.8dB	10^{-4}	15.7dB	10^{-4}	-dB	10^{-4}	15.7dB	10^{-4}	15.8dB
$N = 32, M = 128$	10^{-1}	2.5dB	10^{-1}	2.5dB	10^{-1}	2.6dB	10^{-1}	2.5dB	10^{-1}	2.4dB
$N = 32, M = 128$	10^{-2}	6.5dB	10^{-2}	7dB	10^{-2}	7.1dB	10^{-2}	7.2dB	10^{-2}	7.3dB
$N = 32, M = 128$	10^{-3}	8.8dB	10^{-3}	9.7dB	10^{-3}	9.8dB	10^{-3}	9.5dB	10^{-3}	9.5dB
$N = 32, M = 128$	10^{-4}	9.8dB	10^{-4}	11.3dB	10^{-4}	11.5dB	10^{-4}	11dB	10^{-4}	11dB
$N = 64, M = 128$	10^{-1}	9.8dB	10^{-1}	10dB	10^{-1}	10.1dB	10^{-1}	10.1dB	10^{-1}	10.1dB
$N = 64, M = 128$	10^{-2}	14dB	10^{-2}	15dB	10^{-2}	15dB	10^{-2}	15.1dB	10^{-2}	15.3dB
$N = 64, M = 128$	10^{-3}	16dB	10^{-3}	17.8dB	10^{-3}	17.8dB	10^{-3}	18dB	10^{-3}	18dB
$N = 64, M = 128$	10^{-4}	17.4dB	10^{-4}	18.5dB	10^{-4}	18.5dB	10^{-4}	18.6dB	10^{-4}	18.7dB

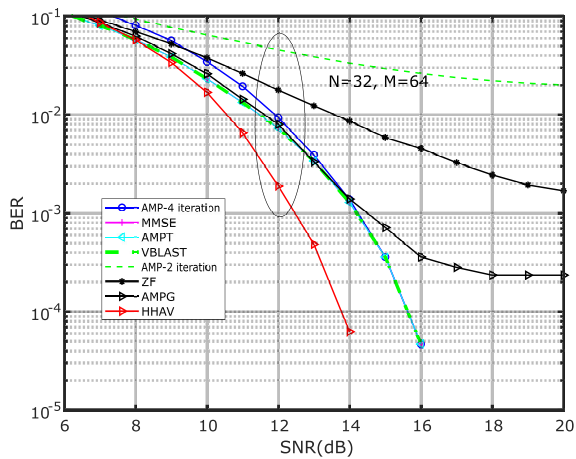


FIGURE 5. An illustration of BER performance of decoding algorithms in a 32 x 64 Massive MIMO system with QPSK modulation scheme.

whereas AMP (AMP-4 iteration) and AMP(T) exhibit identical results.

Finally, we examine the performance of our proposed HHAV algorithm with relatively large constellation size. We also simulate aforementioned algorithms in the said configuration for the comparison. Fig. 7 illustrates the SNR(dB) versus BER performances of various algorithms using the antenna configuration $N \times M = 64 \times 128$ with QPSK modulation scheme. Simulation results show that the performances of AMP(G) and AMP(T) become almost comparable, whereas, as the size of the system grows, our proposed HHAV algorithm improves BER significantly. Comparison of BER performances of HHAV, AMP (4-iteration), AMP(G), AMP(T), and VBLAST schemes in terms of number of users and number of receiving antennas is shown in table2.

IV. FUTURE RESEARCH DIRECTIONS

A considerable work in terms of detection algorithms and their optimization for massive MIMO has been done over the years. It is yet to be seen which algorithm will work

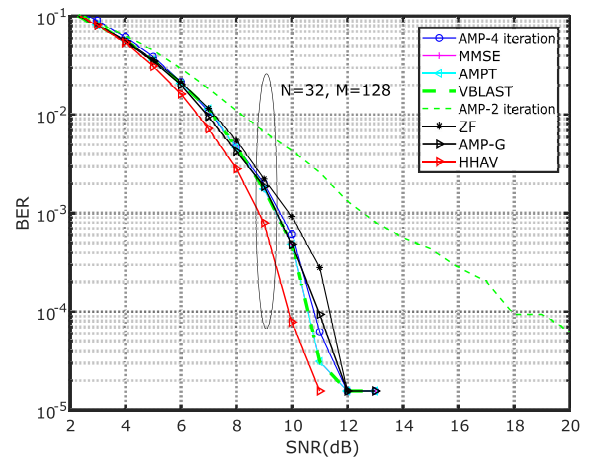


FIGURE 6. An illustration of BER performance of decoding algorithms in a 32 x 128 Massive MIMO system with QPSK modulation scheme.

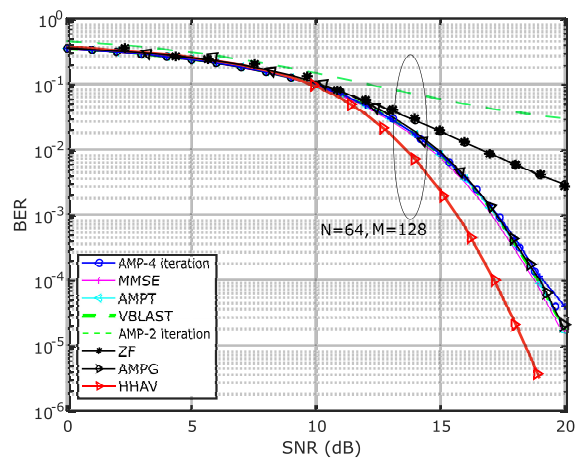


FIGURE 7. An illustration of BER performance of decoding algorithms in a 64 x 128 Massive MIMO system with QPSK modulation scheme.

optimally in practice. If we evaluate massive MIMO in the perspective of future 5G and beyond technologies, the concept of distributed massive MIMO needs to be further

explored. The current research has just focused on collocated radios associated with a single antenna array, whereas, massive MIMO communication systems with centralized elements offer numerous benefits therefore, further investigations are required in the domain of antenna arrays such as extremely large aperture arrays, which will facilitate in achieving the concepts of cell-free massive MIMO, coordinated multipoint, radio stripes, and network MIMO. Few applications such as audio and video streaming are delay sensitive, decoding schemes with minimal delay are required to be developed. Additionally, innovative message passing algorithms with efficient techniques to transfer data with their employment to Iterative detection and decoding (IDD) techniques should be explored. It is anticipated that future 5G networks will consist of multiple and small cells therefore, detection algorithms require schemes with little channel state information from nearby cells and minimal decoding delay. Massive MIMO should also be combined with practical systems such as LTE which will be a promising technology for 5G wireless systems. Moreover, combination of these technologies will assist in designing innovative schemes and will prove to be an appropriate direction for research. In our work, we consider each user with single antenna. However, it will be worthwhile to investigate the scenario in which each user is equipped with many antennas. Furthermore, transmission schemes at BS and decoding schemes at user end and investigation on transceiver designs and evaluation of performance parameters such as data rate, outage probability, of massive MIMO systems with multiple antennas at user end should also be investigated.

V. CONCLUSION

In this paper, we have proposed a novel hybrid scheme viz: HHAV for signal detection in massive MIMO system. It has been proved that the proposed scheme makes a significant difference over various existing detection schemes. Recent AMP algorithm has also been discussed alongwith Ternary and Gaussian distribution functions. It is proved through extensive simulations (we carried out 1000 iterations to confirm results) that our proposed hybrid algorithm can achieve near optimal performance with low complexity. Some existing linear and non-linear detection algorithms, such as ZF, MMSE, and VBLAST have also been reviewed and studied in several scenarios of concern. However, our proposed algorithm outperforms the efficiency and effectiveness of aforementioned algorithms. Furthermore, in our scheme the number of required iterations are small and does not increase with the system dimension to achieve near optimal performance.

REFERENCES

- [1] A. K. Sah, and A. K. Chaturvedi, "An MMP-based approach for detection in large MIMO systems using sphere decoding," *IEEE Wireless Commun. Lett.*, vol. 6, no. 2, pp. 158–161, Apr. 2017.
- [2] F. Rusek, D. Persson, B. K. Lau, E. G. Larsson, T. L. Marzetta, O. Edfors, and F. Tufvesson, "Scaling up MIMO: Opportunities and challenges with very large arrays," *IEEE Signal Process. Mag.*, vol. 30, no. 1, pp. 40–60, Jan. 2013.
- [3] S. Wu, L. Kuang, Z. Ni, J. Lu, D. Huang, and Q. Guo, "Low-complexity iterative detection for large-scale multiuser MIMO-OFDM systems using approximate message passing," *IEEE J. Sel. Topics Signal Process.*, vol. 8, no. 5, pp. 902–915, Oct. 2014.
- [4] S. K. Mohammed, A. Zaki, A. Chockalingam, and B. S. Rajan, "High-rate space-time coded large-MIMO systems: Low-complexity detection and channel estimation," *IEEE J. Sel. Topics Signal Process.*, vol. 3, no. 6, pp. 958–974, Dec. 2009.
- [5] T. L. Marzetta, "Noncooperative cellular wireless with unlimited numbers of base station antennas," *IEEE Trans. Wireless Commun.*, vol. 9, no. 11, pp. 3590–3600, Nov. 2010.
- [6] N. Srinidhi, T. Datta, A. Chockalingam, and B. S. Rajan, "Layered tabu search algorithm for large-MIMO detection and a lower bound on ML performance," *IEEE Trans. Commun.*, vol. 59, no. 11, pp. 2955–2963, Nov. 2011.
- [7] P. Som, T. Datta, N. Srinidhi, A. Chockalingam, and B. S. Rajan, "Low-complexity detection in large-dimension MIMO-ISI channels using graphical models," *IEEE J. Sel. Topics Signal Process.*, vol. 5, no. 8, pp. 1497–1511, Dec. 2011.
- [8] T. Datta, N. Srinidhi, A. Chockalingam, and B. S. Rajan, "A hybrid RTS-BP algorithm for improved detection of large-MIMO M-QAM signals," in *Proc. Nat. Conf. Commun. (NCC)*, Jan. 2011, pp. 1–5.
- [9] W. Feng, Y. Wang, N. Ge, J. Lu, and J. Zhang, "Virtual MIMO in multi-cell distributed antenna systems: Coordinated transmissions with large-scale CSIT," *IEEE J. Sel. Areas Commun.*, vol. 31, no. 10, pp. 2067–2081, Oct. 2013.
- [10] J. Hoydis, S. T. Brink, and M. Debbah, "Massive MIMO in the UL/DL of cellular networks: How many antennas do we need?" *IEEE J. Sel. Areas Commun.*, vol. 31, no. 2, pp. 160–171, Feb. 2013.
- [11] C. Studer and E. G. Larsson, "PAR-aware large-scale multi-user MIMO-OFDM downlink," *IEEE J. Sel. Areas Commun.*, vol. 31, no. 2, pp. 303–313, Feb. 2013.
- [12] M. Musolesi, "Big mobile data mining: Good or evil?" *IEEE Internet Comput.*, vol. 18, no. 1, pp. 78–81, Jan./Feb. 2014.
- [13] A. Morales, R. Alcarria, D. Martin, and T. Robles, "Enhancing evacuation plans with a situation awareness system based on end-user knowledge provision," *Sensors*, vol. 14, no. 6, pp. 11153–11178, 2014.
- [14] L. Atzori, A. Iera, and G. Morabito, "SIoT: Giving a social structure to the Internet of Things," *IEEE Commun. Lett.*, vol. 15, no. 11, pp. 1193–1195, Nov. 2011.
- [15] S. Chen and J. Zhao, "The requirements, challenges, and technologies for 5G of terrestrial mobile telecommunication," *IEEE Commun. Mag.*, vol. 52, no. 5, pp. 36–43, May 2014.
- [16] P. W. Wolniansky, G. J. Foschini, G. D. Golden, and R. A. Valenzuela, "V-BLAST: An architecture for realizing very high data rates over the rich-scattering wireless channel," in *Proc. URSI Int. Symp. Signals, Syst., Electron. Conf.*, vol. 98, Oct. 1998, pp. 295–300.
- [17] X.-X. Xia, Q.-X. Chu, and J.-F. Li, "Design of a compact wideband MIMO antenna for mobile terminals," *Prog. Electromagn. Res. C*, vol. 41, pp. 163–174, 2013.
- [18] C. B. Peel, B. M. Hochwald, and A. L. Swindlehurst, "A vector-perturbation technique for near-capacity multiantenna multiuser communication—Part I: Channel inversion and regularization," *IEEE Trans. Commun.*, vol. 53, no. 1, pp. 195–202, Jan. 2005.
- [19] B. M. Hochwald, C. B. Peel, and A. L. Swindlehurst, "A vector-perturbation technique for near-capacity multiantenna multiuser communication-part II: Perturbation," *IEEE Trans. Commun.*, vol. 53, no. 3, pp. 537–544, Mar. 2005.
- [20] D. Micciancio and S. Goldwasser, *Complexity of Lattice Problems*. Boston, MA, USA: Springer, 2002.
- [21] E. Agrell, T. Eriksson, A. Vardy, and K. Zeger, "Closest point search in lattices," *IEEE Trans. Inf. Theory*, vol. 48, no. 8, pp. 2201–2214, Aug. 2002.
- [22] C. Masouros, M. Sellathurai, and T. Ratnarajah, "Computationally efficient vector perturbation precoding using thresholded optimization," *IEEE Trans. Signal Process.*, vol. 61, no. 5, pp. 1880–1890, May 2013.
- [23] C. Masouros, M. Sellathurai, and T. Ratnarajah, "Maximizing energy efficiency in the vector precoded MU-MISO downlink by selective perturbation," *IEEE Trans. Wireless Commun.*, vol. 13, no. 9, pp. 4974–4984, Sep. 2014.
- [24] D. A. Karpuk and P. Moss, "Channel pre-inversion and max-SINR vector perturbation for large-scale broadcast channels," *IEEE Trans. Broadcast.*, vol. 63, no. 3, pp. 494–506, Sep. 2017.

- [25] Y. Ma, A. Yamani, N. Yi, and R. Tafazolli, "Low-complexity MU-MIMO nonlinear precoding using degree-2 sparse vector perturbation," *IEEE J. Sel. Areas Commun.*, vol. 34, no. 3, pp. 497–509, Mar. 2016.
- [26] D. L. Donoho, A. Maleki, and A. Montanari, "Message-passing algorithms for compressed sensing," *Proc. Nat. Acad. Sci. USA*, vol. 106, no. 45, pp. 18914–18919, 2009.
- [27] D. L. Donoho, A. Maleki, and A. Montanari, "Message passing algorithms for compressed sensing: I. Motivation and construction," *CoRR*, Nov. 2009.
- [28] M. Bayati and A. Montanari, "The dynamics of message passing on dense graphs, with applications to compressed sensing," *IEEE Trans. Inf. Theory*, vol. 57, no. 2, pp. 764–785, Feb. 2011.
- [29] M. Bayati, M. Lelarge, and A. Montanari, "Universality in polytope phase transitions and message passing algorithms," *Ann. Appl. Probab.*, vol. 25, no. 2, pp. 753–822, 2015.
- [30] C. Jeon, R. Ghods, A. Maleki, and C. Studer, "Optimality of large MIMO detection via approximate message passing," in *Proc. IEEE Int. Symp. Inf. Theory (ISIT)*, Jun. 2015, pp. 1227–1231.
- [31] C. Jeon, A. Maleki, and C. Studer, "On the performance of mismatched data detection in large MIMO systems," in *Proc. IEEE Int. Symp. Inf. Theory*, Jul. 2016, pp. 180–184.
- [32] S. Lyu and C. Ling, "Hybrid vector perturbation precoding: The blessing of approximate message passing," *IEEE Trans. Signal Process.*, vol. 67, no. 1, pp. 178–193, Jan. 2019.
- [33] S. Lin and B. W. Kernighan, "An effective heuristic algorithm for the traveling-salesman problem," *Oper. Res.*, vol. 21, pp. 498–516, Mar./Apr. 1973.
- [34] B. W. Kernighan and S. Lin, "An efficient heuristic procedure for partitioning graphs," *Bell Syst. Tech. J.*, vol. 49, no. 2, pp. 291–307, Feb. 1970.
- [35] M. M. Kamruzzaman, W. He, and X. Peng, "Performance of capacity-based adaptive STBC-VBLAST MIMO wireless communication," *Int. J. Wireless Mobile Comput.*, vol. 8, no. 4, pp. 339–345, 2015.
- [36] C. Guo, "Compressed sensing with approximate message passing: Measurement matrix and algorithm design," Ph.D. dissertation, Univ. Edinburgh, Edinburgh, Scotland, 2013.
- [37] S. Rangan, P. Schniter, A. K. Fletcher, and S. Sarkar, "On the convergence of approximate message passing with arbitrary matrices," *IEEE Trans. Inf. Theory*, vol. 65, no. 9, pp. 5339–5351, Sep. 2019.
- [38] M. Khumalo, W.-T. Shi, and C.-K. Wen, "Fixed-point implementation of approximate message passing (AMP) algorithm in massive MIMO systems," *Digit. Commun. Netw.*, vol. 2, no. 4, pp. 218–224, Nov. 2016.
- [39] F. Krzakala, M. Mézard, F. Sausset, Y. Sun, and L. Zdeborová, "Probabilistic reconstruction in compressed sensing: Algorithms, phase diagrams, and threshold achieving matrices," *J. Stat. Mech., Theory Exp.*, vol. 2012, Aug. 2012, Art. no. P08009.
- [40] P. Xiao, W. Yin, C. Cowan, and V. Fusco, "VBLAST detection algorithms utilizing soft symbol estimate and noncircular CAI," *IEEE Trans. Signal Process.*, vol. 59, no. 5, pp. 2441–2447, May 2011.



KIRAN KHURSHID received the B.E. and M.S. degrees in electrical engineering from the National University of Sciences and Technology, Islamabad, Pakistan, in 2007 and 2009 respectively, where she is currently pursuing the Ph.D. degree.

She is a Faculty Member of the Department of Electrical Engineering, APCOMS, Rawalpindi, Pakistan. Her research interests include MIMO systems, massive MIMO systems, wireless channel modeling, and big data mining.



IMRAN RASHID received the B.E. degree in electrical engineering from the National University of Sciences and Technology, Islamabad, Pakistan, in 1999, the M.S. degree in telecommunication engineering (optical communication) from the Technical University of Denmark (Danish: Danmarks Tekniske Universitet), in 2004, and the Ph.D. degree in mobile communication from the University of Manchester, U.K., in 2011.

He is currently the Chief Instructor of the Engineering Wing with the National University of Sciences and Technology. His research interests include mobile and wireless communication, MIMO systems, MU-MIMO systems, compressed sensing for MIMO OFDM systems, massive MIMO systems, M2M for mobile systems, cooperative communication systems, cognitive radio systems, RFID security protocols, and information security for wireless and mobile systems.



ADNAN AHMED KHAN received the B.E. degree in electrical engineering from the University of Engineering and Technology, Lahore, Pakistan, in 1994, the M.S. degree in computer engineering with specialization in networks and communications from the University of Engineering and Technology, Taxila, Pakistan, and the Ph.D. degree in computer engineering from the Center of Advanced Studies in Engineering (CASE) affiliated with the University of Engineering and Technology.

He is currently the Head of the Department of Computer Software Engineering, National University of Sciences and Technology, Islamabad, Pakistan. His research interests include MIMO systems, cooperative communication systems, cognitive spectrum sensing, compressed sensing, wireless channel modeling, and satellite communications.



MUHAMMAD HAROON SIDDIQUI was born in Rawalpindi, Pakistan, in 1974. He received the B.E. and M.S. degrees in electrical engineering from the National University of Sciences and Technology, Islamabad, Pakistan, in 2002 and 2010, respectively, where he is currently pursuing the Ph.D. degree.

He is currently a Faculty Member of the Department of Electrical Engineering, National University of Sciences and Technology. His research

interests include MIMO systems, massive MIMO systems, cooperative communication systems, cognitive spectrum sensing, and wireless channel modeling.



KHUBAIB AHMED received the B.Sc. degree in maths and physics from the University of Punjab, Lahore, Pakistan, in 2000, the M.Sc. degree in electronics from Quaid-i-Azam University, Islamabad, Pakistan, in 2003, and the M.S. degree in computer engineering from the University of Engineering and Technology, Taxila, Pakistan, in 2006.

He is currently a Lecturer with the Department of Physics, COMSATS University Islamabad, Islamabad, Pakistan. His research interests

include massive MIMO systems, cooperative communication systems, cognitive spectrum sensing, and wireless channel modeling.

...